PHYSICAL REVIEW D **88,** 022002 (2013)

Realistic filter cavities for advanced gravitational wave detectors

M. Evans, L. Barsotti, and P. Kwee
Massachusetts Institute of Technology, Cambridge, Massachusetts 02139, USA

J. Harms
INFN, Sezione di Firenze, Sesto Fiorentino 50019, Italy

H. Miao
California Institute of Technology, Pasadena, California 91125, USA
(Received 9 May 2013; published 29 July 2013)

The ongoing global effort to detect gravitational waves continues to push the limits of precision measurement while aiming to provide a new tool for understanding both astrophysics and fundamental physics. Squeezed states of light offer a proven means of increasing the sensitivity of gravitational wave detectors, potentially increasing the rate at which astrophysical sources are detected by more than 1 order of magnitude. Since radiation pressure noise plays an important role in advanced detectors, frequency-dependent squeezing will be required. In this paper we propose a practical approach to producing frequency-dependent squeezing for Advanced Laser Interferometer Gravitational-Wave Observatory (LIGO) and similar interferometric gravitational wave detectors. This work focuses on ''realistic filter cavities'' in the sense that optical losses in the filter cavity and squeezed light source consistent with current technology are considered. The filter cavity solution proposed for Advanced LIGO is ''practical'' in that it considers the nonquantum noise and readout scheme of the interferometer and a potential implementation geometry in the Advanced LIGO vacuum envelope.

DOI: 10.1103/PhysRevD.88.022002 PACS numbers: 04.80.Nn, 42.50.Dv, 04.30.−w, 42.50.Lc

I. INTRODUCTION

The Laser Interferometer Gravitational-Wave Observatory (LIGO) is part of a global effort to directly detect gravitational waves, which has the potential to revolutionize our understanding of both astrophysics and fundamental physics [1–4]. To realize this potential fully, however, significant improvements in sensitivity will be needed beyond Advanced LIGO and similar detectors [5,6].

The use of squeezed states of light (known simply as ''squeezing'') offers a promising direction for sensitivity improvement and has the advantage of requiring minimal changes to the detectors currently under construction [7–10]. Squeezing in advanced detectors will require that the squeezed state be varied as a function of frequency to suppress both the low-frequency radiation pressure noise and the high-frequency shot noise [11–13]. When a squeezed state is reflected off a detuned optical cavity, the frequency-dependent amplitude and phase response of the cavity can be used to vary the squeezed state as a function of frequency. Though all future detectors plan to reduce quantum noise through squeezing, uncertainty remains with respect to the design and limitations of the resonant optical cavities, known as ''filter cavities,'' this will require [14,15].

In this paper we propose a practical approach to producing frequency-dependent squeezing as required by advanced interferometric gravitational-wave detectors. Section II describes the impact of squeezing and filter cavities in the context of a detector with realistic thermal noise, preparing us for a down selection among filter cavity topologies. Section III goes on to suggest a filter cavity implementation appropriate for Advanced LIGO in light of realistic optical losses and other practical factors.

Finally, in the Appendix we introduce a new approach to computing the quantum noise performance of interferometers with filter cavities in the presence of multiple sources of optical loss. This new technique is designed to provide a simple means of generating numerical results and as such does not provide an equation for a given optical configuration, but rather a technique for computing the quantum noise of *any* configuration.

II. QUANTUM NOISE FILTERING IN ADVANCED GRAVITATIONAL-WAVE DETECTORS

The quantum mechanical nature of light sets fundamental constraints on our ability to use it as a measurement tool, and in particular it produces a noise floor in interferometric position measurements like those employed by gravitational-wave detectors. Figure 1 shows the expected sensitivity of an Advanced LIGO-like detector, in which quantum noise is dominant at essentially all frequencies (see in the Appendix for a calculation method and parameters).

The injection of a squeezed vacuum state into an interferometer can reduce quantum noise, as demonstrated in GEO600 and LIGO [9,10]. The ''frequency-independent'' form of squeezing used in these demonstrations will *not*, however, result in a uniform sensitivity improvement in an

advanced detector. The difference comes from the expectation that radiation pressure noise will play a significant role in advanced detectors, and squeezing reduces shot noise at the expense of increased radiation pressure noise (see Fig. 1).

These demonstration experiments focused on reducing quantum noise at high frequency, where shot noise dominates, giving results similar to increasing the total power circulating in the detector (reduced shot noise and increased radiation pressure noise). Increasing circulating power, however, leads to significant technical difficulties related to thermal lensing and parametric instabilities [5,16]. Furthermore, squeezing offers a means of reducing the quantum noise at *any frequency* simply by rotating the squeezed quadrature relative to the interferometer signal quadrature (known as the "squeeze angle") [17]. In general, the squeeze angle that minimizes quantum noise varies as a function of frequency, and a technique for producing the optimal angle at *all frequencies* is required to make effective use of squeezing. One such technique is to reflect a frequency-independent squeezed state off of a detuned Fabry–Perot cavity, known as a "filter cavity" [12]. Figure 2 shows a simplified interferometer with a squeezed light source and a filter cavity.

There are two primary options for the use of filter cavities to improve the sensitivity of advanced gravitational-wave detectors; rotation of the squeezed vacuum state before it enters the interferometer, known as "input filtering;" and rotation of the signal and vacuum state as they exit the interferometer, known as "variational readout" or "output filtering" [12,17,18]. While variational readout appears to have great potential [14,19], a comprehensive study of input and output filtering in the presence of optical losses found that they result in essentially indistinguishable detector performance [15]. In the following sections, we consider the implications of these two approaches in the context of the gravitational wave detectors currently under construction, where filter cavities are likely to be used for the first time.

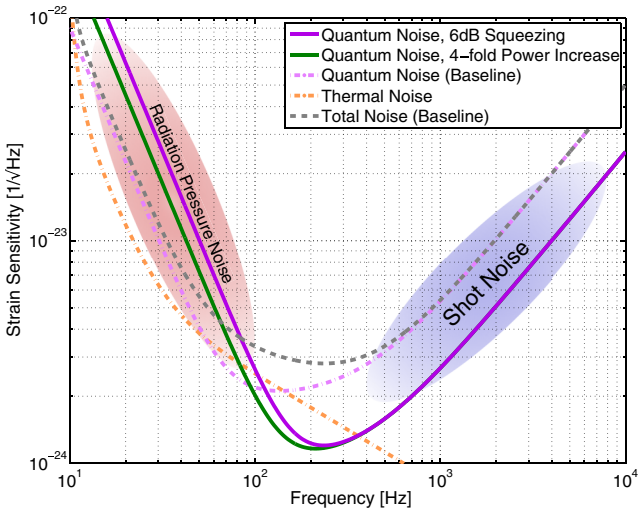

FIG. 1 (color online). The sensitivity of an Advanced LIGO-like detector, our baseline (see Table I for parameters), is limited at most frequencies by quantum noise, though at low frequencies thermal noise also contributes significantly (all other fundamental noise sources are less significant). In terms of quantum noise, 6 dB of squeezing is equivalent to a 4-fold increase in light power circulating in the interferometer, though always somewhat worse at low frequencies due to the degradation of the squeezed vacuum state by optical losses and technical noises [28]. All of the curves in this paper assume 5% injection loss (e.g., from the squeezed vacuum source to the interferometer) and 10% readout loss (e.g., from the interferometer to the readout, including the photodetector quantum efficiency).

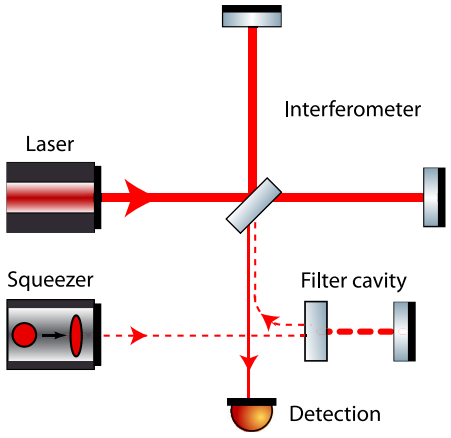

FIG. 2 (color online). A broadband squeezed vacuum state of light with a frequency-dependent squeezing angle can be produced with the help of a filter cavity. Shown here is a simplified interferometer with a linear "input filter cavity" [12].

III. FILTERING SOLUTION FOR ADVANCED LIGO

In this section we propose a *realistic* filter cavity arrangement for implementation as an upgrade to Advanced LIGO. The elements of realism which drive this proposal are the level of thermal noise and mode of operation expected in Advanced LIGO; the geometry of the Advanced LIGO vacuum envelope; and achievable values for optical losses in the squeezed field injection chain, in the filter cavity, and in the readout chain. Furthermore, the scenario considered is that of a near-term upgrade, so significant improvements to other sources of noise in the interferometer are not expected, though it should be noted that the proposed solution is compatible with, and would in fact encourage, a reduction in thermal noise.[1]

While frequency-dependent squeezing for a general signal recycled interferometer requires two filter cavities, only one filter cavity is required to obtain virtually optimal results for a wide-band interferometer that is operated on resonance (i.e., in a "tuned" or "broadband" configuration) [15,21]. Since this is likely to be the primary

[1]A similar study has been conducted for the Einstein Telescope, a proposed future gravitational-wave detector [20].

operating state of Advanced LIGO, we will start by restricting our analysis to this configuration.

Practically speaking, input filtering has the advantage of being functionally separate from the interferometer readout. That is, input filtering can be added to a functioning gravitational-wave detector without modification, and even after it is added, its use is elective. The same cannot be said for output filtering, which requires that a filter cavity be inserted into the interferometer's readout chain. Furthermore, variational readout is incompatible with current readout schemes which produce a carrier field for homodyne detection by introducing a slight offset into the differential arm length, essentially requiring that the homodyne readout angle matches the signal at zero frequency, which is orthogonal to the angle required by variational readout [12,22,23].

The essentially identical performance of input and output filtering, especially in the presence of realistic thermal noise, combined with the practical implications of both schemes push us to select a *single input filter cavity* as a the preferred option. That said, the requirements which drive input and output filter cavity design are very similar such that given a compatible readout scheme the input filter cavity solution presented here can also be used as an output filter cavity.

The impact of losses on cavity line width is inversely proportional to cavity length, and thus it is always the *loss per unit length* that determines filter cavity performance (see Ref. [15] for a detailed discussion). Figure 3 shows that decreasing the round-trip loss below 1 ppm/m will not dramatically improve the detector's sensitivity because of

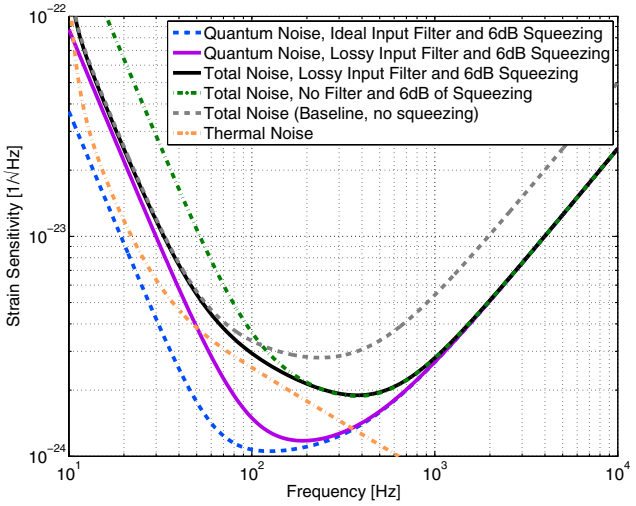

FIG. 3 (color online). Frequency-dependent squeezing decreases both shot noise and radiation pressure noise, reducing quantum noise at all frequencies (blue curve). A lossy filter cavity has degraded performance in the radiation pressure dominated region relative to an ideal lossless filter cavity (purple curve; see Table I for parameters). The lossy filter shown here, with 1 ppm/m round-trip loss, represents a significant advantage over frequency-independent squeezing in that it prevents an *increase* in radiation pressure noise (green dashed curve; see Fig. 1). Furthermore, since thermal noise is significant in the region where radiation pressure noise acts, there is little to be gained by making a lower loss filter cavity in the context of a near-term upgrade to Advanced LIGO.

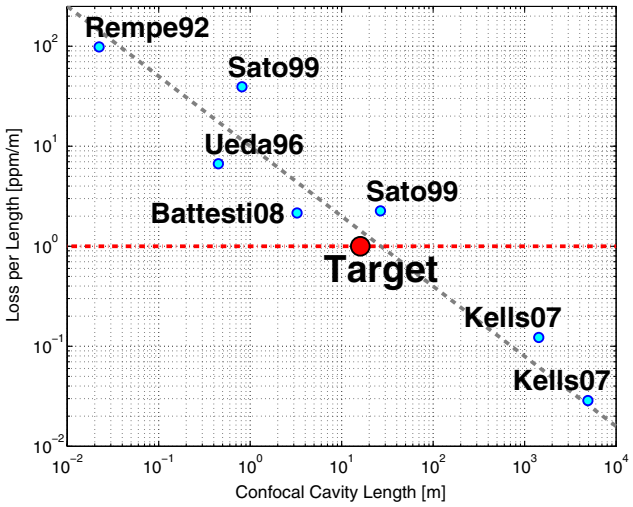

FIG. 4 (color online). Measured round-trip loss per length from the literature [29–33]. Losses grow with beam size on the optics, so a confocal geometry is optimal for minimizing losses and is a good choice for a filter cavity [34]. To remove any dependence on the choice of cavity geometry in the experiments presented here, the beam sizes on the optics are used to scale the cavity length to that of an equivalent confocal cavity. A rough fit to these data is included to guide the eye, and our target value of 1 ppm/m in a 16 m cavity is marked.

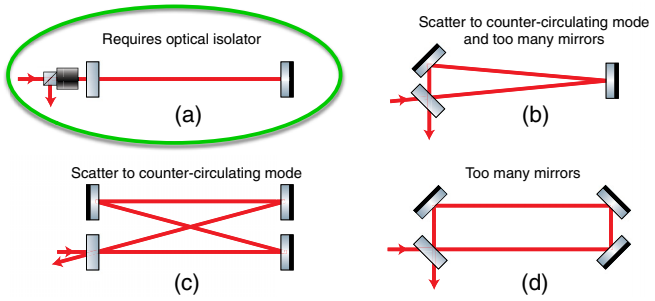

FIG. 5 (color online). Various geometries considered for implementing a filter cavity. Factors considered in choosing among these geometries were cavity length per mirror, potential for scatter into a countercirculating mode, mode quality degradation due to large angle reflection from curved optics, and the ease of separating incident and reflected fields. While a linear cavity (option A) requires an optical isolator to separate input and output fields, it has the best length per mirror, no counter circulating mode, and good mode quality. A polarization based optical isolator will introduce about 1% loss in the squeezed field injection, but this is outside of the filter cavity and modest compared to the 5% estimated total injection loss. For short filter cavities, in which the separation between input and output beams is significant in a bow-tie geometry (C), the coupling to a countercirculating mode may be negligible, and the absence of an optical isolator will make this option preferable.

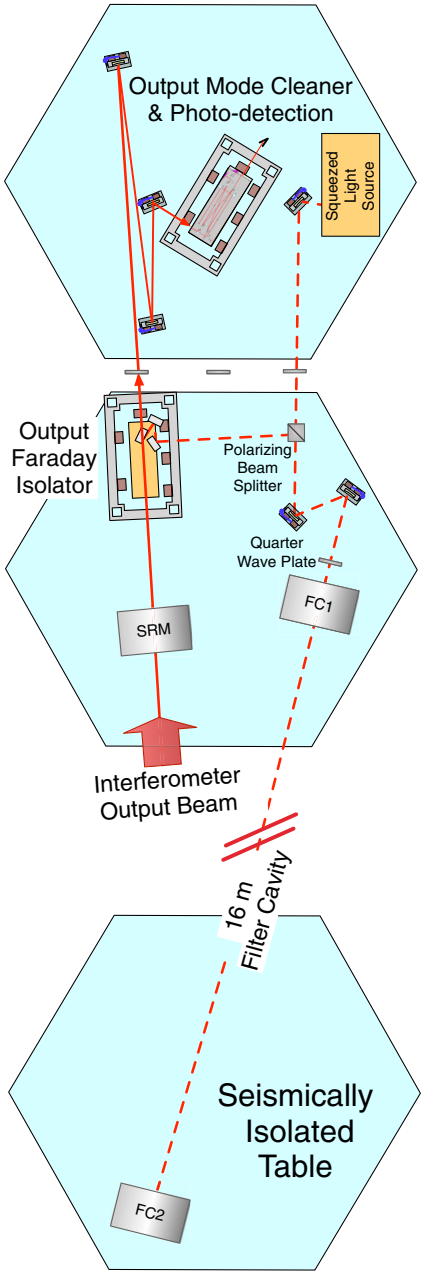

FIG. 6 (color online). An input filter cavity could be included in the existing vacuum envelope of Advanced LIGO. The seismically isolated tables shown in this figure contain the interferometer output optics and offer a 16 m baseline with superior vibration isolation and direct access to the Faraday isolator with which the squeezed vacuum will be injected. Acronyms used in the figure are signal recycling mirror (SRM), filter cavity input mirror (FC1), and filter cavity end mirror (FC2).

the presence of thermal noise, so we take this as the target for an Advanced LIGO filter cavity. While losses below this target have already been demonstrated for kilometer-scale cavities, a study of optical losses in high finesse cavities as a function of cavity length will be required to determine if this is realizable in shorter cavities (see Fig. 4).

To achieve this loss target, it is important to choose a filter cavity geometry which minimizes losses. A *2-mirror linear cavity* with an isolator is a better choice than the 3-mirror triangular geometry frequently used to represent filter cavities [12,15,24] since they both have essentially the same length while the linear cavity has fewer reflections and thus lower loss (see Fig. 5 for details and Ref. [20] for a more detailed discussion).

Looking to a near-term upgrade of Advanced LIGO, the implementation of a short filter cavity which can be housed in the existing vacuum envelope will make squeezing a very attractive option. Since loss per unit length is observed to decrease with cavity length, it is advantageous to make a filter cavity as long as possible. The largest usable distance between two vacuum chambers that house the readout optics in the main experimental hall of Advanced LIGO is about 16 m (see Fig. 6), which is plausibly sufficient to achieve the desired 1 ppm/m loss target.

Several technical issues in the implementation of a filter cavity for Advanced LIGO remain to be addressed before a precise performance prediction can be made. In addition to measurements of the dependence of optical loss on cavity length, the impact of spatial mode mismatch and other sources of loss will need to be carefully evaluated. An analysis of technical noises which degrade filter cavity performance, especially via noise in the reflection phase of the filter cavity, will also be required. Lastly, a detailed control scheme which fixes the length of the filter cavity to produced the desired detuning, will be necessary and is the subject of ongoing research by the authors.

IV. CONCLUSIONS

Squeezed vacuum states offer a proven means of enhancing the sensitivity of gravitational wave detectors, potentially increasing the rate at which astrophysical sources are detected by more than 1 order of magnitude [9,10]. However, due to radiation pressure noise, advanced detectors pose a more difficult problem than the proof-of-principle experiments conducted to date, and narrow line-width optical cavities will be required to make effective use of squeezing.

This work adds to previous efforts, which were aimed at parametrizing optimal filter cavity configurations in the context of a generalized interferometric gravitational-wave detector by identifying a practical and effective filter cavity design for Advanced LIGO and similar interferometric detectors. We find that a 2-mirror linear cavity with 1 ppm/m round-trip loss is sufficient to reap much of the benefit that squeezing can provide. Quantitatively speaking, 6 dB of squeezing and an ideal input filter cavity would increase the range at which an Advanced LIGO-like detector could detect a coalescing binary neutron star system by 36% while 6 dB of squeezing and a filter cavity with 1 ppm/m round-trip loss would increase the range by 18%.

Finally, we include a mathematical formalism which can be used to compute quantum noise in the presence of

multiple sources of optical loss. This approach also maps the "audio sideband" or "one-photon" formalism commonly used to compute the behavior of classical fields in interferometers to the two-photon formalism used to compute quantum noise, thereby offering a simple connection between the optical parameters of a system and its quantum behavior.

ACKNOWLEDGMENTS

The authors gratefully acknowledge the support of the National Science Foundation and the LIGO Laboratory, operating under cooperative Agreement No. PHY-0757058. The authors also acknowledge the wisdom and carefully aimed gibes received from Yanbei Chen, Nergis Mavalvala, and Rana Adhikari, all of which helped to motivate and mold the contents of this work. Jan Harms carried out his research for this paper at the California Institute of Technology. This paper has been assigned LIGO Document No. LIGO-P1300054.

APPENDIX: MATHEMATICAL FORMALISM

We use the following mathematical formalism to calculate quantum noise, as shown in Figs. 1 and 3. This treatment is based on Kimble *et al.* [12], Buonanno and Chen [25], and Harms *et al.* [17] (henceforth KLMTV, BnC, and HCF). The notation of HCF is used whenever possible.

This treatment extends HCF to a simple means of including all sources of loss but makes no attempt to find analytic expressions for optimal values for a filter cavity parameter as this appears better done numerically. To simplify the relevant expressions, a transformation from the one-photon formalism to the two-photon formalism is also presented and used for computing the input-output relations of filter cavities.[7]

We start by noting that the output of the interferometer can be written as a sum of signal and noise fields

$$\bar{\mathbf{o}} = \bar{\mathbf{s}}h + \sum_n \mathbf{T_n}\bar{\mathbf{i}}_\mathbf{n}, \tag{A1}$$

where $\bar{\mathbf{o}}$ is the output field, $\bar{\mathbf{s}}$ h the output signal field generated by a gravitational-wave strain h, and $\mathbf{T_n}\bar{\mathbf{i}}_\mathbf{n}$ the transfer matrix and source term for the nth noise field. [Relative to Eq. (2) in HCF, the prefactor $1/M$ is absorbed into $\mathbf{T_n}$ and $\bar{\mathbf{s}}$ to make the terms more independent, and we have allowed for multiple noise fields as suggested in the text preceding their Eq. (1).] In this notation each $\bar{\mathbf{i}}_\mathbf{n}$ is a coherent vacuum field of the two-photon formalism such that

$$\bar{\mathbf{i}}_\mathbf{n} = \begin{pmatrix}\alpha_1 & \alpha_2\end{pmatrix}, \qquad \alpha_1 = \begin{pmatrix}1\\0\end{pmatrix}, \qquad \alpha_2 = \begin{pmatrix}0\\1\end{pmatrix}, \tag{A2}$$

where α_1 and α_2 represent the two field quadratures [7,26]. Thus, for N vacuum fields entering an interferometer $\{\bar{\mathbf{i}}_\mathbf{1}, \ldots, \bar{\mathbf{i}}_\mathbf{N}\}$, there are $2N$ independent noise sources.

Carrying this through to the noise spectral density [HCF Eq. (7)] gives

$$S_h = \frac{\sum_n |\bar{\mathbf{b}}_\zeta \cdot \mathbf{T_n}|^2}{|\bar{\mathbf{b}}_\zeta \cdot \bar{\mathbf{s}}|^2}, \tag{A3}$$

where we have kept the homodyne field vector $\bar{\mathbf{b}}_\zeta$ as in BnC. To avoid ambiguity, in our notation the dot product of vectors $\bar{\mathbf{a}} \cdot \bar{\mathbf{b}} \equiv \langle \mathbf{a}|\mathbf{b}\rangle \equiv \sum_n a_n^* b_n$ is a complex number, the dot product of a vector and a matrix $\bar{\mathbf{a}} \cdot \mathbf{B} \equiv \langle \mathbf{a}|\mathbf{B} \equiv \bar{\mathbf{a}}^\dagger \mathbf{B}$ is a vector, and the magnitude squared of a vector $|\bar{\mathbf{a}}|^2 \equiv \sum_n |a_n|^2$ is a real number.

In Eq. (A3), each $\mathbf{T_n}$ is a 2×2 transfer matrix which takes the coherent vacuum field $\bar{\mathbf{i}}_\mathbf{n}$ from its point of entry into the interferometer to the readout photodetector. The transfer matrix $\mathbf{T_1}$ for vacuum fluctuations from the squeezed light source, for instance, can be constructed by taking a product of transfer matrices

$$\mathbf{T_1} = \mathbf{T_{ro}}\mathbf{T_{ifo}}\mathbf{T_{inj}}S(r, \lambda), \tag{A4}$$

where $S(r, \lambda)$ is the operator for squeezing by e^r with angle λ, $\mathbf{T_{inj}}$ takes the squeezed field from its source to the interferometer, $\mathbf{T_{ifo}}$ is the input-output transfer matrix of the interferometer ($\mathbf{C}/M$ in BnC and $\mathbf{T}/M$ in HCF), and $\mathbf{T_{ro}}$ transfers the field from the interferometer to the readout. In the case of input filtering, $\mathbf{T_{inj}}$ will impose a frequency-dependent rotation of the squeeze angle, while for output filtering, $\mathbf{T_{ro}}$ will rotate the noise and signal fields as they propagate to the photodetector.

Computation of the input-output relation for any optical system can be performed in the two-photon formalism [27] or in the simpler audio-sideband "one-photon" picture where the transfer of a field at frequency $\omega_0 + \Omega$ is given by $\tau(\Omega)$ (as in previous works, ω_0 is the carrier frequency and Ω the signal sideband frequency). To convert between pictures, we define transfer coefficients for positive and negative sidebands as $\tau_+ = \tau(\Omega)$ and $\tau_- = \tau(-\Omega)$ and then compute the two-photon transfer matrix as

$$\mathbf{T} = A_2 \begin{pmatrix}\tau_+ & \\ & \tau_-^*\end{pmatrix} A_2^{-1}, \quad A_2 = \frac{1}{\sqrt{2}}\begin{pmatrix}1 & 1\\ -i & +i\end{pmatrix}. \tag{A5}$$

Off-diagonal elements in the one-photon transfer matrix are unnecessary for filter cavities since those elements represent nonlinear transformations that couple the positive and negative sideband amplitudes such as squeezing or radiation pressure backaction.

For a filter cavity, the one-photon transfer coefficient is just the amplitude reflectivity of the cavity,

$$r_{\mathrm{fc}}(\Omega) = r_{\mathrm{in}} - \frac{t_{\mathrm{in}}^2}{r_{\mathrm{in}}} \frac{r_{\mathrm{rt}} e^{-i\phi(\Omega)}}{1 - r_{\mathrm{rt}} e^{-i\phi(\Omega)}}, \tag{A6}$$

where the cavity round-trip reflectivity r_{rt} is related to its bandwidth by

$$\gamma_{\rm fc} = -\log(r_{\rm rt}) f_{\rm FSR} \simeq \frac{1-r_{\rm rt}^2}{2} f_{\rm FSR}, \quad f_{\rm FSR} = \frac{c}{2L_{\rm fc}}, \tag{A7}$$

and the round-trip phase derives from the cavity detuning according to

$$\phi(\Omega) = \frac{\Omega - \Delta\omega_{\rm fc}}{f_{\rm FSR}}, \qquad \Delta\omega_{\rm fc} = \omega_{\rm fc} - \omega_0 \tag{A8}$$

for a cavity of length $L_{\rm fc}$ and resonant frequency $\omega_{\rm fc}$. (The cavity "bandwidth" is the half-width of the resonance, a.k.a. the "cavity pole" frequency. In KLMTV the detuning is given in terms of the bandwidth $\xi = \Delta\omega_{\rm fc}/\gamma_{\rm fc}$.) The amplitude reflectivity of the cavity input-output coupler is related to its transmissivity by $r_{\rm in}^2 \le 1 - t_{\rm in}^2$ and to the round-trip reflectivity by $r_{\rm rt} \le r_{\rm in}$, where a lossless filter cavity attains equality in both expressions. The filter cavity transfer matrix in the two-photon formalism is

$$\mathbf{T_{fc}} = A_2 \begin{pmatrix} r_{\rm fc+} & \\ & r_{\rm fc-}^* \end{pmatrix} A_2^{-1}. \tag{A9}$$

Returning to an interferometer with input filtering, and including injection and readout losses, we can write

$$\bar{\mathbf{s}} = L(\Lambda_{\rm ro})\bar{\mathbf{s}}_0 \tag{A10}$$

$$\mathbf{T_{in1}} = L(\Lambda_{\rm ro})\mathbf{T_{ifo}}\mathbf{T_{fc}}L(\Lambda_{\rm inj})S(r,\lambda) \tag{A11}$$

$$\mathbf{T_{in2}} = L(\Lambda_{\rm ro})\mathbf{T_{ifo}}\mathbf{T_{fc}}\Lambda_{\rm inj} \tag{A12}$$

$$\mathbf{T_{in3}} = L(\Lambda_{ro})\mathbf{T_{ifo}}\Lambda_{\rm fc} \tag{A13}$$

$$\mathbf{T_{in4}} = \Lambda_{\rm ro}, \tag{A14}$$

where $L(\Lambda_x) = \sqrt{1-\Lambda_x^2}$ is the transfer coefficient of a power loss Λ_x^2. The four $\mathbf{T_n}$ terms each contribute to the sum in Eq. (A3) since each represents an entry point for coherent vacuum fluctuations [12]. $\mathbf{T_{in1}}$ propagates the squeezed field from its source to the photodetector, and $\mathbf{T_{in2}}$ accounts for the losses of the injection path (from squeezer to filter cavity). $\mathbf{T_{in3}}$ represents the frequency dependent losses in the filter cavity with

$$\Lambda_{\rm fc}^2 = 1 - (|r_{\rm fc+}|^2 + |r_{\rm fc-}|^2)/2. \tag{A15}$$

Finally, $\mathbf{T_{in4}}$ accounts for losses in the readout path, from interferometer to photodetector including the detector quantum efficiency.

For an interferometer with output filtering, on the other hand, we have

$$\bar{\mathbf{s}} = L(\Lambda_{\rm ro})\mathbf{T_{fc}}\bar{\mathbf{s}}_0 \tag{A16}$$

$$\mathbf{T_{out1}} = L(\Lambda_{\rm ro})\mathbf{T_{fc}}\mathbf{T_{ifo}}L(\Lambda_{\rm inj})S(r,\lambda) \tag{A17}$$

TABLE I. Symbols and values.

Symbol	Meaning	Value
c	Light speed	299 792 458 m/s
ω_0	Frequency of carrier field	$2\pi \times 282$ THz
$P_{\rm bs}$	Power on the beam splitter	5.6 kW
m	Mass of each test-mass mirror	40 kg
$L_{\rm arm}$	Arm cavity length	3995 m
$L_{\rm src}$	Signal cavity length	55 m
$\gamma_{\rm arm}$	Arm cavity half-width	$2\pi \times 42$ Hz
$t_{\rm sr}^2$	Signal mirror power transmission	35%
$\Lambda_{\rm inj}^2$	Injection losses	5%
$\Lambda_{\rm ro}^2$	Readout losses	10%
$t_{\rm in}^2$	Filter cavity input transmission	
	Ideal 16 m filter cavity	66 ppm
	1 ppm/m loss 16 m filter cavity	50 ppm
$\gamma_{\rm fc}$	Filter cavity half-width	$2\pi \times 49$ Hz
$\Delta\omega_{\rm fc}$	Filter cavity detuning	$2\pi \times 49$ Hz

$$\mathbf{T_{out2}} = L(\Lambda_{\rm ro})\mathbf{T_{fc}}\mathbf{T_{ifo}}\Lambda_{\rm inj} \tag{A18}$$

$$\mathbf{T_{out3}} = L(\Lambda_{\rm ro})\Lambda_{\rm fc} \tag{A19}$$

$$\mathbf{T_{out4}} = \Lambda_{\rm ro}, \tag{A20}$$

where the signal produced by the interferometer $\bar{\mathbf{s}}_0$ is modified by the filter cavity, in addition to experiencing some loss in the readout process.

The transfer matrix and signal vector for a tuned signal recycled interferometer of the sort discussed in Sec. III and analyzed in Sec. III.C.2 of BnC are

$$\mathbf{T_{ifo}} = \begin{pmatrix} 1 & \mathcal{K}_{\rm sr} \\ 0 & 1 \end{pmatrix}, \qquad \bar{\mathbf{s}}_0 = \frac{\sqrt{2\mathcal{K}_{\rm sr}}}{h_{\rm SQL}} \begin{pmatrix} 1 \\ 0 \end{pmatrix}, \tag{A21}$$

where

$$h_{\rm SQL} = \sqrt{\frac{8\hbar}{mL_{\rm arm}^2\Omega^2}}, \qquad \mathcal{K}_{\rm sr} = \frac{\mathcal{K}t_{\rm sr}^2}{|1 + e^{2i\Phi}r_{\rm sr}|^2}, \tag{A22}$$

$$\mathcal{K} = \frac{8P_{\rm bs}\omega_0}{mL_{\rm arm}^2\Omega^2(\Omega^2 + \gamma_{\rm arm}^2)}, \tag{A23}$$

$$\Phi = \Omega L_{\rm src}/c + \arctan(\Omega/\gamma_{\rm arm}), \tag{A24}$$

and the signal recycling mirror amplitude reflectivity and transmissivity are $r_{\rm sr}$ and $t_{\rm sr}$ for consistency with Eqs. (A6)–(A9) (these are ρ and τ in BnC and HCF). Symbol definitions, and the values used in our calculations, are given in Table I.

[1] LIGO Laboratory, "LIGO web site," http://www.ligo.caltech.edu/.

[2] Virgo Collaboration, "Virgo web site," http://wwwcascina.virgo.infn.it/.

[3] KAGRA, "KAGRA web site," http://gwcenter.icrr.u-tokyo.ac.jp/.

[4] GEO600, "GEO web site," http://www.geo600.org/.

[5] G. M. Harry and the LIGO Scientific Collaboration, Classical Quantum Gravity **27**, 084006 (2010).

[6] LIGO Scientific Collaboration, "GWIC Roadmap," https://gwic.ligo.org/roadmap/.

[7] C. M. Caves and B. L. Schumaker, Phys. Rev. A **31**, 3068 (1985).

[8] R. Schnabel, N. Mavalvala, D. E. McClelland, and P. K. Lam, Nat. Commun. **1**, 121 (2010).

[9] LIGO Scientific Collaboration, Nat. Phys. **7**, 962 (2011).

[10] J. Aasi *et al.* (LIGO Scientific Collaboration), Nat. Photonics, doi:10.1038/nphoton.2013.177 (2013).

[11] M. T. Jaekel and S. Reynaud, Europhys. Lett. **13**, 301 (1990).

[12] H. Kimble, Y. Levin, A. Matsko, K. Thorne, and S. Vyatchanin, Phys. Rev. D **65**, 022002 (2001).

[13] S. Chelkowski, H. Vahlbruch, B. Hage, A. Franzen, N. Lastzka, K. Danzmann, and R. Schnabel, Phys. Rev. A **71**, 013806 (2005).

[14] D. McClelland, N. Mavalvala, Y. Chen, and R. Schnabel, Laser Photonics Rev. **5**, 677 (2011).

[15] F. Y. Khalili, Phys. Rev. D **81**, 122002 (2010).

[16] M. Evans, L. Barsotti, and P. Fritschel, Phys. Lett. A **374**, 665 (2010).

[17] J. Harms, Y. Chen, S. Chelkowski, A. Franzen, H. Vahlbruch, K. Danzmann, and R. Schnabel, Phys. Rev. D **68**, 042001 (2003).

[18] F. Khalili, Phys. Rev. D **77**, 062003 (2008).

[19] Y. Chen, S. L. Danilishin, F. Y. Khalili, and H. Müller-Ebhardt, Gen. Relativ. Gravit. **43**, 671 (2011).

[20] ET Science Team, "Einstein Gravitational wave Telescope Conceptual Design Study," http://www.et-gw.eu/etdsdocument.

[21] P. Purdue and Y. Chen, Phys. Rev. D **66**, 122004 (2002).

[22] T. T. Fricke, N. D. Smith-Lefebvre, R. Abbott, R. Adhikari, K. L. Dooley, M. Evans, P. Fritschel, V. V. Frolov, K. Kawabe, J. S. Kissel, B. J. J. Slagmolen, and S. J. Waldman, Classical Quantum Gravity **29**, 065005 (2012).

[23] M. Evans, P. Fritschel, and V. V. Frolov, "Low-noise homodyne readout for quantum limited gravitational wave detectors" (in preparation).

[24] F. Khalili, Phys. Rev. D **76**, 102002 (2007).

[25] A. Buonanno and Y. Chen, Phys. Rev. D **64**, 042006 (2001).

[26] H. Yuen, Phys. Rev. A **13**, 2226 (1976).

[27] T. Corbitt, Y. Chen, and N. Mavalvala, Phys. Rev. A **72** (2005).

[28] S. Dwyer *et al.*, "Squeezed quadrature fluctuations in a gravitational wave detector using squeezed light," Opt. Express (to be published).

[29] G. Rempe, R. J. Thompson, H. J. Kimble, and R. Lalezari, Opt. Lett. **17**, 363 (1992).

[30] A. Ueda, N. Uehara, K. Uchisawa, K.-i. Ueda, H. Sekiguchi, T. Mitake, K. Nakamura, N. Kitajima, and I. Kataoka, Opt. Rev. **3**, 369 (1996).

[31] S. Sato, S. Miyoki, M. Ohashi, and M. K. Fujimoto, Appl. Opt. **38**, 2880 (1999).

[32] W. Kells, California Institute of Technology Technical Report LIGO-T070051, 2007 https://dcc.ligo.org/LIGO-T070051.

[33] R. Battesti, B. Pinto Da Souza, S. Batut, C. Robilliard, G. Bailly, C. Michel, M. Nardone, L. Pinard, O. Portugall, G. Trénec, J. M. Mackowski, G. L. J. A. Rikken, J. Vigué, and C. Rizzo, Eur. Phys. J. D **46**, 323 (2008).

[34] F. Magaña-Sandoval, R. X. Adhikari, V. Frolov, J. Harms, J. Lee, S. Sankar, P. R. Saulson, and J. R. Smith, J. Opt. Soc. Am. A **29**, 1722 (2012).